

# Spin-controlled plasmonics via optical Rashba effect

Nir Shitrit, Igor Yulevich, Vladimir Kleiner, and Erez Hasman

Citation: *Appl. Phys. Lett.* **103**, 211114 (2013); doi: 10.1063/1.4832636

View online: <http://dx.doi.org/10.1063/1.4832636>

View Table of Contents: <http://aip.scitation.org/toc/apl/103/21>

Published by the [American Institute of Physics](#)

---

---

**Fearful for the future of science?**

Programs and Resources | Publications | Career Resources | Member Societies | About AIP | [Contact Us](#)

**FYI**  
AMERICAN INSTITUTE OF PHYSICS

on authoritative news and resources

**FYI This Week**  
A newsletter, issued each Monday morning and covers the upcoming week and its focus on the physics community.

**The Week Ahead**  
A weekly app for mobile devices that provides a quick overview of the week's events and opportunities.

**Sign up for FREE FYI emails.**  
AIP American Institute of Physics

FYI Bulletin

## Spin-controlled plasmonics via optical Rashba effect

Nir Shitrit, Igor Yulevich, Vladimir Kleiner, and Erez Hasman<sup>a)</sup>

*Micro and Nanooptics Laboratory, Faculty of Mechanical Engineering, and Russell Berrie Nanotechnology Institute, Technion—Israel Institute of Technology, Haifa 32000, Israel*

(Received 15 September 2013; accepted 7 November 2013; published online 20 November 2013)

Observation of the optical Rashba effect in plasmonics is reported. Polarization helicity degeneracy removal, associated with the inversion symmetry violation, is attributed to the surface symmetry design via anisotropic nanoantennas with space-variant orientations. By utilizing the Rashba-induced momentum in a nanoscale kagome metastructure, we demonstrated a spin-based surface plasmon multidirectional excitation under a normal-incidence illumination. The spin-controlled plasmonics via spinoptical metasurfaces provides a route for spin-based surface-integrated photonic nanodevices and light-matter interaction control, extending the light manipulation capabilities. © 2013 AIP Publishing LLC. [<http://dx.doi.org/10.1063/1.4832636>]

The relativistic spin-orbit coupling phenomena in solids of the spin Hall<sup>1,2</sup> and Rashba effects<sup>3–5</sup> have triggered an enormous interest owing to their potential impact on spintronics.<sup>6</sup> To elaborate, the Rashba effect is a manifestation of the spin-orbit interaction under broken inversion symmetry (i.e., the inversion transformation  $\mathbf{r} \rightarrow -\mathbf{r}$  does not preserve the structure), where the electron spin-degenerate parabolic bands split into dispersions with oppositely spin-polarized states. This effect can be illustrated via a relativistic electron in an asymmetric quantum well experiencing an effective magnetic field in its rest frame, induced by a perpendicular potential gradient  $\nabla V$ , as represented by the spin-polarized momentum offset  $\Delta k \propto \pm \nabla V$ .<sup>3–5</sup> In terms of symmetries, the spin degeneracy associated with the spatial inversion symmetry is lifted due to a symmetry-breaking electric field normal to the heterointerface.

The photonic version of the Rashba effect was recently introduced in spinoptical metamaterials,<sup>7–9</sup> where the spin-orbit interaction of light, i.e., a coupling of the intrinsic angular momentum (photon spin) and the extrinsic momentum,<sup>10,11</sup> generates a spin-polarized momentum correction with a geometric origin.<sup>12–18</sup> Similar to the role of a potential gradient in the electronic Rashba effect, the space-variant orientation angle  $\theta(x, y)$  of anisotropic optical nanoantennas induces a spin-split dispersion of  $\Delta k_R = \sigma \nabla \theta$ ,<sup>7–9</sup> where  $\sigma_{\pm} = \pm 1$  is the photon spin corresponding to right and left circularly polarized light, respectively. The optical Rashba effect (ORE) was observed in the spontaneous emission of anisotropic thermal antenna patterns, such as the quasi one-dimensional antenna array,<sup>7,8</sup> and the inversion asymmetric (IaS) two-dimensional kagome lattice (KL) metamaterial.<sup>9</sup> The Rashba-induced geometric momentum correction can be either added to or subtracted from the light momentum, owing to its spin-dependent origin; in this manner, light-matter interactions governed by momentum selection rules are perturbed. As a result, spinoptical metamaterials introduce the photon helicity as an additional degree of freedom for controlling photonics with the light intrinsic angular momentum as manifested in the optical spin Hall<sup>12–18</sup> and Rashba effects.<sup>7–9</sup>

Surface plasmon polaritons (SPPs) are propagating surface-confined waves arising from the coupling of an electromagnetic field with the collective oscillations of quasi-free electrons at the metal surface.<sup>19</sup> Plasmonic devices can confine light in regions with dimensions that are smaller than the wavelength of the excited photons in free space;<sup>20,21</sup> hence, plasmonic metasurfaces have recently generated a considerable interest owing to their technological impact as the link between conventional optics and integrated on-chip photonics.<sup>22,23</sup> In this context, light manipulation on the nanoscale via electromagnetic surface waves provides the route for state-of-the-art miniaturized devices ushering in photonic nanocircuits. The resonant coupling of light to SPPs via inversion symmetric metastructures is governed by the standard momentum-matching condition; so, once the structural properties are set, the excitation can be tuned by changing the light's wavelength or angle of incidence.<sup>24</sup> Despite this, the ORE enables the engineering of light-matter interactions in a spin-based manner via the lattice symmetry breaking; hence, the ORE-plasmonics alliance holds the promise for controlling SPPs by switching the light intrinsic spin.

In this Letter, we report on the experimental observation of the ORE in nanoscale plasmonics. By designing the meta-surface symmetry properties with space-variant oriented anisotropic nanoantennas, an IaS metastructure was obtained for spin-controlled multidirectional guiding of SPPs under normal-incidence illumination (see Fig. 1(a)). The presented surface-integrated nanoscale device of a plasmonic multiport in the visible spectrum is governed by generalized momentum conservation; this selection rule highlights the additional momentum provided by a geometric Rashba gradient in a spinoptical metamaterial. In agreement with a dispersion analysis of the ORE, we observed the directional distribution of SPP jets via free-space imaging using a circular decoupling slit. Spin-based SPP multidirectional excitation was demonstrated in the anisotropic nanoantenna pattern of the IaS two-dimensional KL. The directed SPP jets depend on both the wavelength and the polarization helicity of the incident light, so for a given wavelength, the jets are spin-controlled. The spin-based surface-wave propagation via the ORE offers symmetry-controlled light-matter interactions,

<sup>a)</sup>Electronic mail: mehasman@technion.ac.il

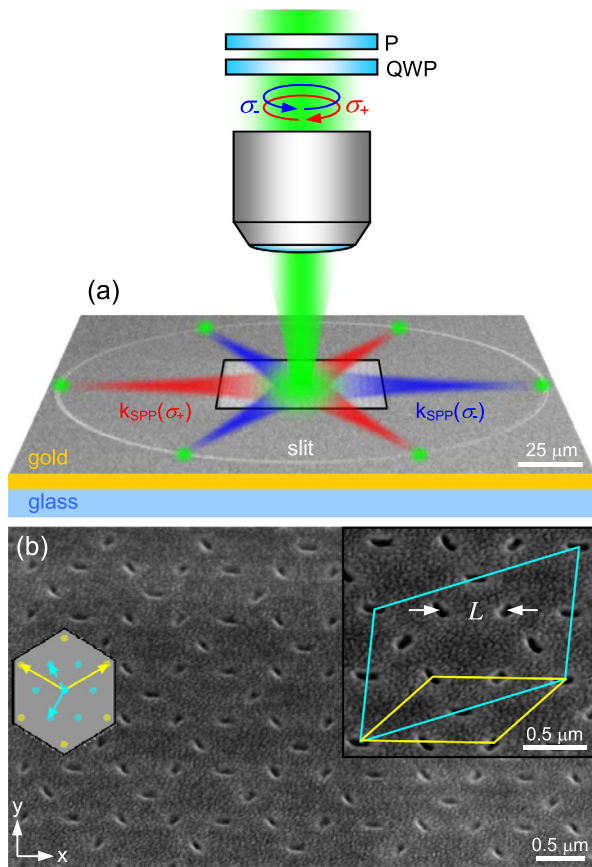


FIG. 1. Spin-controlled plasmonics via the ORE. (a) Schematic setup for spin-based excitation of multidirectional SPP jets arising from the metasurface symmetry breaking. The antenna metasurface depicted by the frame is normally illuminated with a laser light whose polarization is set by a circular polarizer (a linear polarizer (P) followed by a quarter-wave plate (QWP)) and propagating SPPs are free-space imaged with a decoupling slit. (b) Scanning electron microscopy image of the plasmonic  $\sqrt{3} \times \sqrt{3}$  KL. Yellow and blue rhombuses in the right inset show the isotropic and  $\sqrt{3} \times \sqrt{3}$  unit cells in real space, respectively. The left inset depicts the reciprocal space of isotropic and  $\sqrt{3} \times \sqrt{3}$  structures with the corresponding reciprocal vectors. The dashed blue arrow indicates that only one of the  $\sqrt{3} \times \sqrt{3}$  reciprocal vectors is required to set the dispersion of a spinoptical metasurface, in addition to both of the isotropic reciprocal vectors.

thus enabling the realization of custom-tailored spinoptical nanodevices for light manipulation.

As a Rashba-type metasurface, we consider a periodic anisotropic antenna array with a local orientation angle of  $\theta(\mathbf{r}_n)$ , where  $\mathbf{r}_n$  is the position vector of the  $n$ th antenna. Such a superstructure is manifested by two differentiated structural and orientational unit cells, associated with periodicities of the elementary lattice points and the antenna ordering, respectively.<sup>7,9</sup> By exciting space-variant anisotropic nanoantennas, which are linear polarization selective,<sup>8,16</sup> with a circularly polarized light, regarded as a rotating-in-time linear polarization,<sup>14,17</sup> a spin-polarized geometric phase delay of  $\phi_g = -\sigma\theta$  arises.<sup>13,14</sup> Alternatively, this phase can be viewed as the Pancharatnam-Berry phase, where the polarization state at different locations along the metasurface traverses various geodesic paths upon the Poincaré sphere.<sup>25–33</sup> The additional geometric phase, which is not acquired through optical path differences, can be expressed as  $\phi_g = -\sigma\mathbf{K}_R \cdot \mathbf{r}_n$  via the geometrically induced Rashba wavevector of  $-\sigma\mathbf{K}_R = \nabla\phi_g$ , attributed to the periodicity of the vector

field and set by the orientational unit cell. Accordingly, the light-matter interaction of a spinoptical metasurface is perturbed by the spin-orbit coupling, which is the origin of the geometric phase; this ushers in generalized momentum conservation of the spin-orbit momentum-matching (SOMM) condition  $\mathbf{k}_{in}^{\parallel}(\sigma) = \mathbf{k}_{SPP} + m\mathbf{G}_1 + n\mathbf{G}_2 - \sigma\mathbf{K}_R$ , with a spin-dependent geometric correction based on polarization rotation, appearing in addition to the intrinsic structural contribution.<sup>9</sup> Here,  $\mathbf{k}_{in}^{\parallel}$  is the wavevector of the incident light in the surface plane,  $\mathbf{k}_{SPP}$  is the SPP wavevector,  $\mathbf{G}_{1,2}$  are the primitive structural reciprocal vectors, and  $(m, n)$  are the indices of the radiative modes. The spin-based scattering controlled by the SOMM condition is related to Fourier amplitudes  $f(\mathbf{k}, \sigma) = \sum_n e^{i(\mathbf{k} \cdot \mathbf{r}_n - \sigma\theta(\mathbf{r}_n))}$  of the periodic spinoptical metamaterial. In view of this, in an inversion symmetric metastructure, where  $\theta(\mathbf{r}_n) = \theta(-\mathbf{r}_n)$ , spin-degenerated reciprocal space amplitudes of  $|f(\mathbf{k}, \sigma)| = |f(\mathbf{k}, -\sigma)|$  are obtained. However, if the inversion symmetry is broken, the spin degeneracy is removed, and the optical Rashba spin-split dispersion, attributed to the geometric gradient, is observed.<sup>7–9</sup>

A peculiar configuration of a spinoptical metasurface for investigating the ORE is the kagome metastructure. In the geometrically frustrated KL, formed of vertex-sharing triangles, the antiferromagnetic ordering is characterized by competing spin-folding modes showing either uniform or staggered ( $\sqrt{3} \times \sqrt{3}$ ) chirality, associated with structural and magnetic unit cells, respectively.<sup>34</sup> The peculiarity of the KL lies in the different symmetries of the spin structures with respect to spatial inversion, so the reordering of the local magnetic moments transforms the lattice from an inversion symmetric to an asymmetric structure. Hence, as a spin-controlled plasmonic metasurface for observing the ORE, we considered the artificial kagome structure (Fig. 1(b)),<sup>9</sup> with anisotropic nanoantennas geometrically arranged according to the  $\sqrt{3} \times \sqrt{3}$  magnetic kagome phase.<sup>34</sup> The spin-projected dispersion relation  $\omega(k)$  of the IaS KL metamaterial obeys the SOMM condition arising from the combined contributions of the structural and orientational lattices (right inset of Fig. 1(b));<sup>9</sup> hence, SPP jet is excited resonantly when the generalized momentum conservation is fulfilled. In the KL,  $(\mathbf{G}_1, \mathbf{G}_2) = (\pi/L)(\hat{x} + \hat{y}/\sqrt{3}, -\hat{x} + \hat{y}/\sqrt{3})$  are the structural reciprocal vectors determined by the isotropic unit cell, where  $L$  is the nearest-antenna distance. The specific geometric Rashba correction of  $\mathbf{K}_R$  is arbitrarily selected from  $\mathbf{K}_{1,2} = (\pi/3L)(-\hat{x} \mp \sqrt{3}\hat{y})$ , which are the orientational reciprocal vectors, determined by a  $\sqrt{3} \times \sqrt{3}$  unit cell (left inset of Fig. 1(b));<sup>9</sup> based on this choice, the secondary orientational vector linearly depends on the primary  $\mathbf{K}_R$  and both the structural vectors  $\mathbf{G}_{1,2}$ . Considering low modes of  $(m, n) \in \{0, \pm 1\}$ , we calculated the spin-dependent dispersion of the  $\sqrt{3} \times \sqrt{3}$  KL in the IaS direction of the  $x$  axis, revealing the optical Rashba spin-split of  $|\Delta k_R| = 2\pi/3L$  (Fig. 2(a)).

The radiation dispersion of a spinoptical metasurface (Fig. 2(a)) does not directly shed light on the propagation direction of SPPs, which is the essence of spin-controlled plasmonics. Yet, the directional two-dimensional distribution of excited SPPs can be constructed from the vector representation of the SOMM condition. Figure 2(b) presents the vector dispersion of SPPs  $\mathbf{k}_{SPP}(\omega, \mathbf{k}_{in}^{\parallel}, \sigma)$  manifested by the

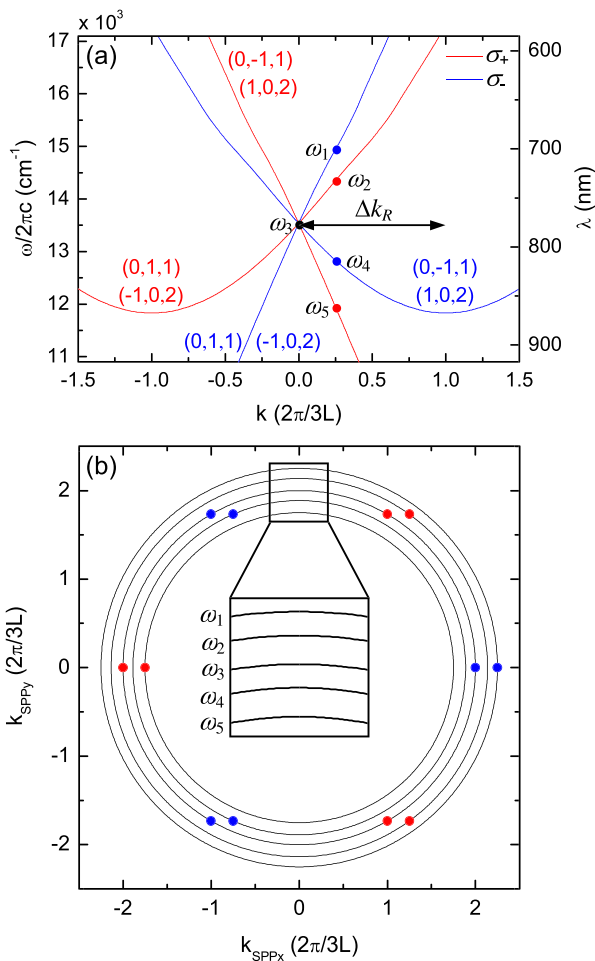


FIG. 2. Spin-split optical Rashba dispersion of a spinoptical metasurface. (a) Spin-projected radiation dispersion of the  $\sqrt{3} \times \sqrt{3}$  KL configuration at the IaS  $x$  direction calculated via the SOMM condition. Red and blue lines correspond to  $\sigma_{\pm}$  incident spin states, respectively. Modes are specified with indices  $(m, n, i)$ , where  $i$  is the index of the specific Rashba correction. (b) Spin-controlled SPP vector dispersion. Circles represent isofrequency curves, where the inset shows the legend of frequencies depicted in (a). Red and blue points correspond to directional SPP wavevectors excited by  $\sigma_{\pm}$ , respectively. The spin degeneracy removal in normal incidence at  $\omega_3$  is observed in the SPP dispersion and not in the radiation dispersion, as manifested by the spin-degenerated black point in (a).

directions of SPP wavevectors along the isofrequency circles. This accompanying representation reveals that degenerated modes in the radiative dispersion give rise to spatially non-degenerated near-field excitations. Explicitly, the time reversal symmetry of  $\omega(k, \sigma_+) = \omega(-k, \sigma_-)$  observed in the radiation dispersion ushers in spin degeneracy of the frequency in normal incidence (i.e.,  $k = 0$ ; see the spin-degenerated black point in Fig. 2(a)). However, the SPP dispersion clearly shows the spin degeneracy removal in surface-wave excitation, resulting in spin-controlled multidirectional plasmonic launching (see the  $\omega_3$  isofrequency circle in Fig. 2(b)). These combined radiative and SPP dispersions serve as a complete set and provide the route for a full characterization of spin-controlled plasmonics via Rashba-type metasurfaces.

In view of this, we fabricated using a focused ion beam (FEI Strata 400s dual beam system, Ga<sup>+</sup>, 30 keV, 48 pA) the KL  $\sqrt{3} \times \sqrt{3}$  plasmonic metasurface consisting of  $80 \times 220 \text{ nm}^2$  rectangular void antennas with  $L = 480 \text{ nm}$ , etched

to a depth of 60 nm into a 200 nm thick gold film, evaporated onto a glass substrate (Fig. 1(b)). The  $60 \mu\text{m}$  square array was surrounded by a circular slit with a diameter of  $180 \mu\text{m}$  and a width of 100 nm, where only the antenna metasurface was normally illuminated with a continuous wave Ti:sapphire tunable laser (Spectra-Physics 3900 S) via a circular polarizer (see Fig. 1(a) for the experimental setup). The resonant illuminating wavelength of 740 nm was set according to the calculated spin-projected dispersion (Fig. 2(a)), and the SPPs excited by the metasurface and decoupled by the slit were free-space imaged. In accordance with the 6-fold rotational symmetry of the  $\sqrt{3} \times \sqrt{3}$  KL and the vector representation of the SOMM condition (Figs. 3(c) and 3(d)), 3 plasmonic jets propagating in  $60^\circ$ ,  $180^\circ$ , and  $300^\circ$  directions were measured for  $\sigma_+$  illumination (Fig. 3(a)); by flipping the spin to  $\sigma_-$  excitation, a mirror image is observed (Fig. 3(b)). The efficiency of the spin-based multidirectional launching was quantitatively characterized by a figure of merit defined as the ratio between the  $\sigma_{\pm}$  intensities measured along the slit (Fig. 3(e)), at a specific preferred direction; high experimental figures of merit of nearly 15 in such a spin-controlled plasmonic metasurface hold the promise for spin-switch multidirectional guiding for surface-integrated multiport nanodevices based on the ORE.

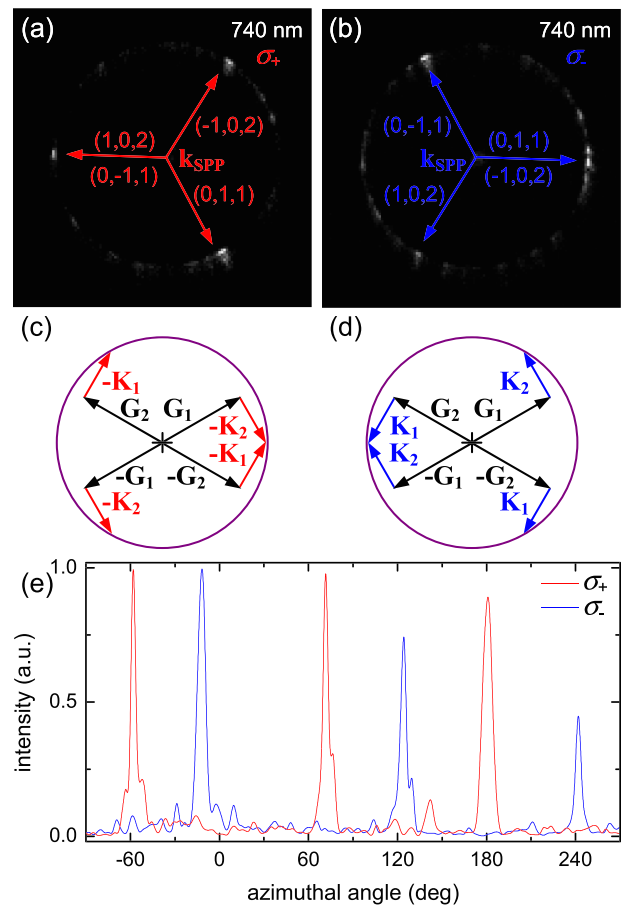


FIG. 3. Experimental observation of the ORE in the plasmonic KL metasurface. (a), (b) Measured intensities of multidirectional SPP jets excited by the KL for  $\sigma_{\pm}$  illuminations, respectively, at a wavelength of 740 nm. (c), (d) Vector summation representation of the SOMM condition for  $\sigma_{\pm}$ , respectively. Note that  $\mathbf{k}_{\text{SPP}}$  is the complementary vector for the origin in the  $\mathbf{k}_{\text{SPP}}$  circle according to the corresponding mode indices. (e) Azimuthal cross sections of the intensity distributions along the slit revealing the spin-controlled multidirectional excitation.



The observed spin-based multidirectional plasmonic launching via the ORE is fundamentally related to intrinsic symmetry properties of the KL metasurface. According to Noether's theorem, for every symmetry there is a corresponding physical conservation law;<sup>35</sup> particularly, invariance with respect to a spatial translation or rotation corresponds to conservation of the linear or angular momentum, respectively. The invariance of higher complex structures, such as the  $\sqrt{3} \times \sqrt{3}$  KL, under a translation followed by a rotation arises in a spin-orbit coupling.<sup>9</sup> When the group theory formalism is applied to consider the KL translation-rotation symmetry constraint, the SOMM selection rule is generated,<sup>9</sup> elucidating the spin-dependent directional distribution of surface-wave jets.

In summary, the ORE was presented in the plasmonic KL metasurface, where the SPP spin-controlled multidirectional guiding was observed. The excitation of different modes in the optical Rashba dispersion results in a directed plasmonic propagation depending on both the wavelength and the spin of the incident light, thus providing a route for combined polarization- and wavelength-based nanodevices. The reported phenomenon harnesses the development of a unified theory to establish a link between a metasurface symmetry breaking and selection rules with extra degrees of freedom to encompass a broader class of light-matter interaction controls. Spinoptical metamaterials offer the realization of state-of-the-art nanoscale devices via the polarization encoding in surface waves, providing an integrated on-chip photonic nanocircuit platform for information processing and optical communication.

This research was partially supported by the Israel Science Foundation and the Israel Nanotechnology Focal Technology Area on Nanophotonics for Detection.

<sup>1</sup>M. I. Dyakonov and V. I. Perel, *Phys. Lett. A* **35**, 459 (1971).

<sup>2</sup>Y. K. Kato, R. C. Myers, A. C. Gossard, and D. D. Awschalom, *Science* **306**, 1910 (2004).

<sup>3</sup>G. Dresselhaus, *Phys. Rev.* **100**, 580 (1955).

<sup>4</sup>E. I. Rashba, *Sov. Phys. Solid State* **2**, 1109 (1960).

<sup>5</sup>K. Ishizaka, M. S. Bahramy, H. Murakawa, M. Sakano, T. Shimojima, T. Sonobe, K. Koizumi, S. Shin, H. Miyahara, A. Kimura, K. Miyamoto, T.

Okuda, H. Namatame, M. Taniguchi, R. Arita, N. Nagaosa, K. Kobayashi, Y. Murakami, R. Kumai, Y. Kaneko, Y. Onose, and Y. Tokura, *Nature Mater.* **10**, 521 (2011).

<sup>6</sup>S. A. Wolf, D. D. Awschalom, R. A. Buhrman, J. M. Daughton, S. von Molnár, M. L. Roukes, A. Y. Chtchelkanova, and D. M. Treger, *Science* **294**, 1488 (2001).

<sup>7</sup>N. Dahan, Y. Gorodetski, K. Frischwasser, V. Kleiner, and E. Hasman, *Phys. Rev. Lett.* **105**, 136402 (2010).

<sup>8</sup>K. Frischwasser, I. Yulevich, V. Kleiner, and E. Hasman, *Opt. Express* **19**, 23475 (2011).

<sup>9</sup>N. Shitrit, I. Yulevich, E. Maguid, D. Ozeri, D. Veksler, V. Kleiner, and E. Hasman, *Science* **340**, 724 (2013).

<sup>10</sup>V. S. Liberman and B. Y. Zel'dovich, *Phys. Rev. A* **46**, 5199 (1992).

<sup>11</sup>N. M. Litchinitser, *Science* **337**, 1054 (2012).

<sup>12</sup>O. Hosten and P. Kwiat, *Science* **319**, 787 (2008).

<sup>13</sup>K. Y. Bliokh, Y. Gorodetski, V. Kleiner, and E. Hasman, *Phys. Rev. Lett.* **101**, 030404 (2008).

<sup>14</sup>Y. Gorodetski, A. Niv, V. Kleiner, and E. Hasman, *Phys. Rev. Lett.* **101**, 043903 (2008).

<sup>15</sup>K. Y. Bliokh, A. Niv, V. Kleiner, and E. Hasman, *Nature Photon.* **2**, 748 (2008).

<sup>16</sup>N. Shitrit, I. Bretner, Y. Gorodetski, V. Kleiner, and E. Hasman, *Nano Lett.* **11**, 2038 (2011).

<sup>17</sup>N. Shitrit, S. Nechayev, V. Kleiner, and E. Hasman, *Nano Lett.* **12**, 1620 (2012).

<sup>18</sup>X. Yin, Z. Ye, J. Rho, Y. Wang, and X. Zhang, *Science* **339**, 1405 (2013).

<sup>19</sup>M. L. Brongersma and V. M. Shalaev, *Science* **328**, 440 (2010).

<sup>20</sup>K. Li, M. I. Stockman, and D. J. Bergman, *Phys. Rev. Lett.* **91**, 227402 (2003).

<sup>21</sup>J. A. Schuller, E. S. Barnard, W. Cai, Y. C. Jun, J. S. White, and M. L. Brongersma, *Nature Mater.* **9**, 193 (2010).

<sup>22</sup>N. I. Zheludev and Y. S. Kivshar, *Nature Mater.* **11**, 917 (2012).

<sup>23</sup>A. V. Kildishev, A. Boltasseva, and V. M. Shalaev, *Science* **339**, 1232009 (2013).

<sup>24</sup>A. Drezet, D. Koller, A. Hohenau, A. Leitner, F. R. Aussenegg, and J. R. Krenn, *Nano Lett.* **7**, 1697 (2007).

<sup>25</sup>S. Pancharatnam, *Proc. Indian Acad. Sci., Sect. A* **44**, 247 (1956).

<sup>26</sup>M. V. Berry, *Proc. R. Soc. London, Ser. A* **392**, 45 (1984).

<sup>27</sup>M. V. Berry, *J. Mod. Opt.* **34**, 1401 (1987).

<sup>28</sup>Z. Bomzon, V. Kleiner, and E. Hasman, *Opt. Lett.* **26**, 1424 (2001).

<sup>29</sup>Z. Bomzon, G. Biener, V. Kleiner, and E. Hasman, *Opt. Lett.* **27**, 1141 (2002).

<sup>30</sup>G. Biener, A. Niv, V. Kleiner, and E. Hasman, *Opt. Lett.* **27**, 1875 (2002).

<sup>31</sup>E. Hasman, V. Kleiner, G. Biener, and A. Niv, *Appl. Phys. Lett.* **82**, 328 (2003).

<sup>32</sup>A. Niv, G. Biener, V. Kleiner, and E. Hasman, *Opt. Commun.* **251**, 306 (2005).

<sup>33</sup>E. Hasman, G. Biener, A. Niv, and V. Kleiner, in *Progress in Optics*, edited by E. Wolf (Elsevier, Amsterdam, 2005), Vol. 47, pp. 215–289.

<sup>34</sup>D. Grohol, K. Matan, J.-H. Cho, S.-H. Lee, J. W. Lynn, D. G. Nocera, and Y. S. Lee, *Nature Mater.* **4**, 323 (2005).

<sup>35</sup>E. Noether, *Nachr. Ges. Wiss. Goettingen, Math.-Phys. Kl.* 235 (1918).